AVALANCHE STATISTICS IN TRANSFER LOAD MODELS OF EVOLVING DAMAGE

Tomasz Derda

Institute of Mathematics, Czestochowa University of Technology, Poland
tomasz.derda@im.pcz.pl

Abstract. The damage evolution occurring in a set of elements in the nodes of the supporting one- and two-dimensional lattices is analysed within the stochastic Fibre Bundle Model approach. The element-strength-thresholds are drawn from a given probability distribution and the set of elements is subjected to an external load that is increased quasi-statically. If an element fails, its load has to be transferred to the other intact elements. We compare avalanche statistics i.e. the number of damaged elements for three different load transfer protocols, namely the global, local and recently introduced so-called Voronoi load transfer rule. Our example system is an array of nanopillars.

Introduction

The knowledge of fracture evolution up to global rupture and its effective description are important for the analysis of the transport processes occurring in heterogeneous media. From the theoretical point of view, the understanding of the complexity of the rupture process has advanced due to the use of lattice models. An example of great importance is the family of transfer load models, especially Fibre Bundle Models (FBM) [1-21]. In a static FBM, a set of fibres is located in the nodes of the supporting lattice and the element-strength-thresholds are drawn from a given probability distribution. After an element has failed, its load has to be transferred to the other intact elements. Two extreme cases are: global load sharing (GLS, also known as equal load sharing - ELS) - the load is equally shared by the remaining elements and local load sharing (LLS) - only the neighbouring elements suffer from the increasing load.

In this work, apart from the aforementioned transfer rules, we employ an approach based on Voronoi polygons - the extra load is equally redistributed among the elements lying inside the Voronoi regions generated by a group of elements destroyed within an interval of time taken to be the time step. We call this load transfer rule Voronoi load sharing (VLS). This kind of load transfer not only merges the GLS and LLS approach concepts but also induces supplemental randomness to the model. It is because of the fact that the number of intact elements inside of a particular Voronoi region is random.

Voronoi polygons are one of the most fundamental and useful constructs defined by irregular lattices [22]. For set $\mathbf{X} = \{x_1, x_2, ..., x_N\}$ of N distinct points in $\Omega \subset \mathbf{R}^2$, the Voronoi tessellation is the partition of Ω into N polygons denoted by ΔV_i. Each ΔV_i is defined as the set of points which are closer to x_i than to any points in $\mathbf{X}$. All of the Voronoi regions are convex polygons. In Figure 1, an example of Voronoi polygons is shown, in the case of square-shaped pillars.
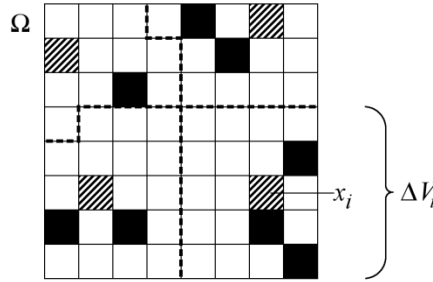

Fig. 1. Voronoi polygons for set of square-shaped pillars: white squares-intact pillars, black squares-previously destroyed pillars and shaded squares-just damaged pillars

1. Load transfer modelling

Consider an array of N mechanically independent pillars located in the nodes of the lattice. In this work we are concerned with both one-dimensional lattices and two-dimensional square lattices. To each pillar x_i we assign a critical load (in the sense of a strength-threshold) σ_{th}^i which is randomly distributed according to distribution $P(\sigma_{th})$, $i = 1, 2, \mathrm{K}, N$. When load σ_i applied on the pillar attains σ_{th}^i, the pillar crashes. In this work we employ uniform distribution of pillar strength-thresholds with the probability and density functions: $P(\sigma_{th}) = \sigma_{th}$, $p(\sigma_{th}) = 1$, respectively. The strength-thresholds values are drawn from interval [0,1].

1.1. Loading of the system

Starting with all intact pillars, which corresponds to a zero load, we load the system by growing external force F until the whole array of pillars collapses. This external load F is the control parameter of the model. The set of pillars is loaded in a *quasi-static* way. The system is uniformly loaded until the weakest intact pillar fails and the increase of the load stops. After this failure, the actual load coming from the crashed pillar is transferred to the other intact pillars according to a given transfer rule. The increased stress on the intact pillars may give rise to

another failures, after which the load transfer from the destroyed elements may cause subsequent failures *etc*. If the load transfer does not provoke further failures there is a stable configuration and external load F has to be increased until the weakest remaining pillar crashes. The above described procedure is repeated till the system completely fails. Once the stress on the pillar attains its strength-threshold value, the pillar is instantaneously and irreversibly damaged.

2. Appearance of avalanches and their evolution

The number of damaged pillars under an equal external load is called an avalanche (Δ), hence the avalanche is the number of destroyed pillars between two consecutive load increments. In other words, the avalanche is the number of crashed pillars between one stable state and the next stable state.

We study the distribution of the avalanche sizes appearing during the entire breakdown process. Calculations have been done for three types of load transfer rules, namely, GLS, VLS and LLS, including different variants of the LLS model. We realised simulations for two system sizes: $N = 400 \times 400$ pillars and $N = 10^4$ pillars. These simulations are time consuming, especially for large systems, thus the statistics built up for a system of size $N = 10^4$ pillars is better than that for its bigger counterpart.

Let $D(\Delta)$ denote the number of avalanches of size Δ. Figures 2-4 illustrate the avalanche size distribution on a single sample for the GLS, VLS and LLS rules, respectively. The system consists of $N = 400 \times 400$ pillars. As we can see, the avalanche distribution for the GLS and VLS rules is very similar.
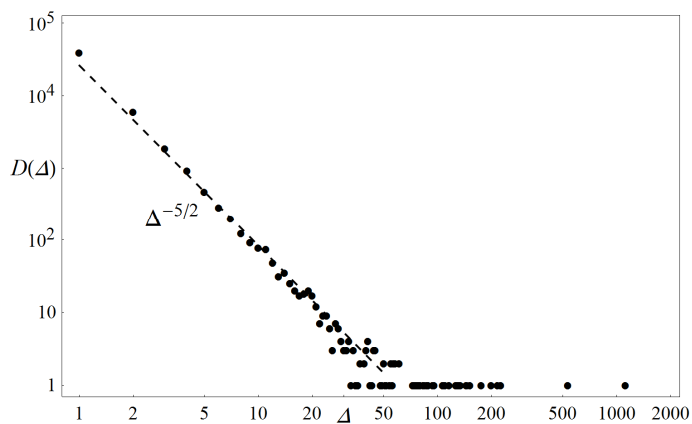

Fig. 2. Avalanche size distribution for GLS. Figure is based on single sample containing $N = 400 \times 400$ pillars
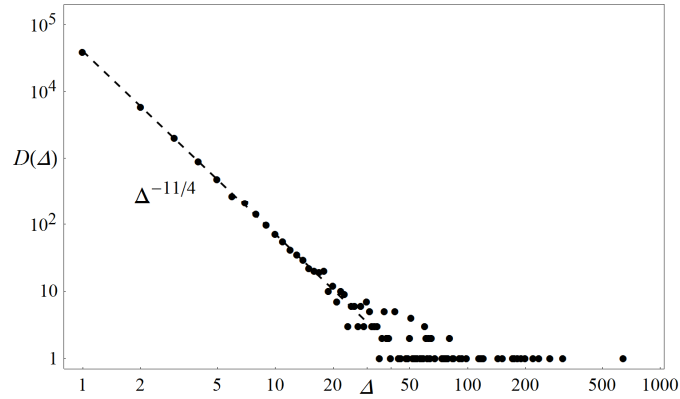
Fig. 3. Avalanche size distribution in 2D system for VLS rule. Figure is based on single sample containing $N = 400 \times 400$ pillars
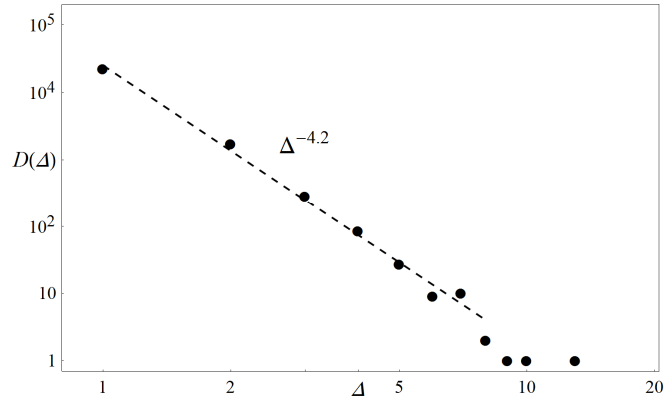

Fig. 4. Avalanche size distribution in 2D system for LLS rule. Figure is based on single sample containing $N = 400 \times 400$ pillars

The distribution of avalanches for the GLS rule follows a universal power law:

$$D(\Delta) \propto \Delta^{-\alpha} \tag{1}$$

where exponent $\alpha = 5/2$ [3-5]. For the VLS rule, we obtained exponent value $\alpha \approx 11/4$. The characteristic of the LLS avalanche distribution is completely different. For small-size avalanches, the LLS apparently has a power law distribution with a much bigger value of $\alpha \approx 4.2$ [4].

Next, we consider the following quantities for the different transfer rules:
–   average number of avalanches
–   mean critical stresses
–   average size of catastrophic avalanche

The results, shown in Table 1 are based on 1000 simulations performed for a system size of $N = 10^4$ pillars.

The number of avalanches accounts for the number of load increase steps till the whole system is completely damaged. As we can see, the biggest number of steps of load increase occurs for both the GLS and VLS rules. The damage process for the LLS rule runs in a much smaller number of steps of load increase. With respect to the variants of the LLS rule, it can be noticed that the bigger the number of neighbours to which load is passed (from damaged pillars) the greater the number of avalanches.

Table 1

Statistics of damaging process for GLS, VLS and different variants of LLS. Results are based on 1000 samples, each containing $N = 10\ 000$ pillars. Abbreviations: st. - standard LLS, n - nearest neighbour, r - right neighbour, l - left neighbour

Load transfer rules			Average number of avalanches	Mean critical stress $\langle \sigma_c \rangle = \langle F_c \rangle / N$	Mean critical stress $\langle \sigma_{fa} \rangle = \langle F_c \rangle / \langle \Delta_{fa} \rangle$	Average size of cata-strophic avalanche $\langle \Delta_{fa} \rangle$
GLS			3081.8	0.2507	0.5005	5009
2D VLS			3079.3	0.2505	0.4956	5054
LLS	2D	st.	1839.8	0.1654	0.2102	7866
		1n	1138.3	0.1070	0.1220	8771
		2n	1206.0	0.1127	0.1297	8687
		3n	1876.4	0.1683	0.2157	7803
		4n	1934.0	0.1727	0.2237	7720
		5n	2060.9	0.1826	0.2423	7536
	1D	1r	1102.5	0.1036	0.1176	8812
		1r 1l	1313.6	0.1220	0.1425	8563
		1n	1118.2	0.1052	0.1196	8794
		2n	1445.7	0.1333	0.1587	8397

We define two quantities of critical stress related to
– initial number of pillars $\sigma_c = F_c / N$
– size of catastrophic avalanche $\sigma_{fa} = F_c / \Delta_{fa}$

where F_c is the total critical load causing a complete breakdown of the system. The values of the critical stress for GLS and VLS rules are very similar. For these transfer load rules, the system is able to sustain a much bigger external load with respect to the one corresponding to the LLS scheme. The results for variants of the LLS scheme indicate that the average system strength increases as the number of

neighbours to which the load is passed grows. An increase in the number of neighbours to which the load is passed enables the system to sustain a greater external load. In general, one can say that the bigger the number of intact pillars which receive the load from damaged pillars (transferred load is more dispersed), the bigger the external load the system can support before a complete breakdown.

Critical load F_c triggers a catastrophic avalanche Δ_{fa}, i.e. a final avalanche breaking all the remaining pillars and causes a macroscopic failure of the entire system, so the final stage of the breakdown process. The average size of a catastrophic avalanche $\left\langle \Delta_{fa} \right\rangle$ is reported in Table 1 and it is seen that for the GLS rule, the catastrophic avalanche starts when on average almost half of the pillars is destroyed. For the VLS rule, the mean size of the final catastrophic avalanche is slightly bigger than for the GLS rule. In the case of the LLS scheme the mean size of the catastrophic avalanche is much bigger in comparison to the GLS and VLS rules, so that the final avalanche for the LLS rule occurs at an earlier stage of the breakdown process. Concerning the variants of the LLS rule, we see that the bigger the number of neighbours to which the load is passed, the smaller the mean size of the catastrophic avalanche.

Figures 5-7 show the avalanche distribution for the GLS, VLS and LLS rules, respectively. The results are based on 1000 simulations on a system of size $N = 10^4$ pillars. Similarly to the results of the above analysed single sample, the avalanche distributions for the GLS and VLS rules follow power law behaviour with exponents $\alpha = 5/2$ and $\alpha \approx 2.65$ respectively.

The distribution of avalanches for the LLS rule yields $\alpha \approx 3.9$ which means that this load transfer procedure represents the strongest way of system destruction.
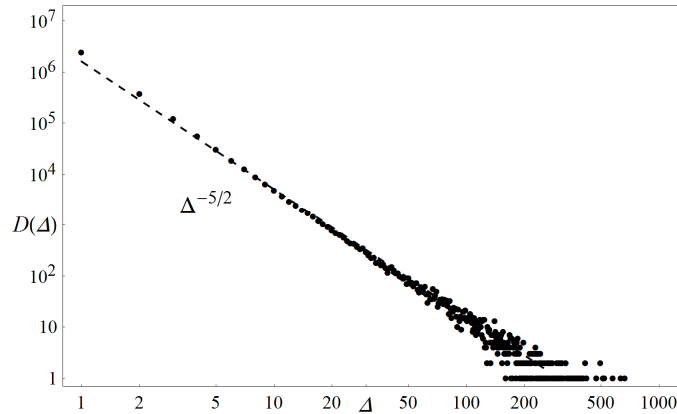

Fig. 5. Avalanche size distribution for GLS. Figure is based on 1000 samples, each containing $N = 100 \times 100$ pillars
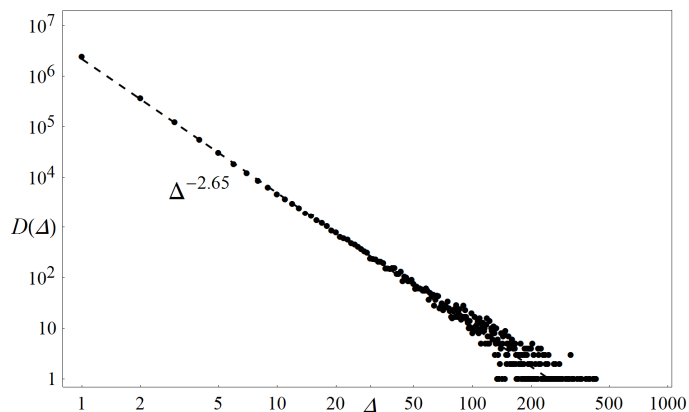
Fig. 6. Avalanche size distribution in 2D system for VLS rule. Figure is based
on 1000 samples, each containing $N = 100 \times 100$ pillars
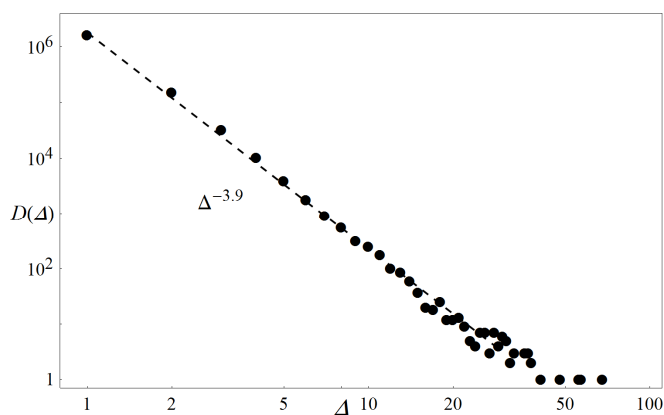

Fig. 7. Avalanche size distribution in 2D system for LLS rule. Figure is based
on 1000 samples, each containing $N = 100 \times 100$ pillars

In Figure 8, we compare the avalanche distributions for the LLS rule in a one-dimensional system. As can be seen, the distribution for small-size avalanches apparently follows a power law with exponents $\alpha \approx 4.2$ and $\alpha \approx 4.5$. When the load is transferred to the two nearest neighbours the model is characterised by a greater number of avalanches of a given size in comparison to a model to load transfer to a single nearest neighbour.

Figure 9 illustrates the avalanche distributions for two-dimensional variants of the LLS model. We obtained two separate runs of avalanche distribution: one for variants transferring load to a maximum number of two neighbours (exponent $\alpha \approx 4.5$) and the second for variants transferring load to three or more neighbours (exponent $\alpha \approx 3.8$).
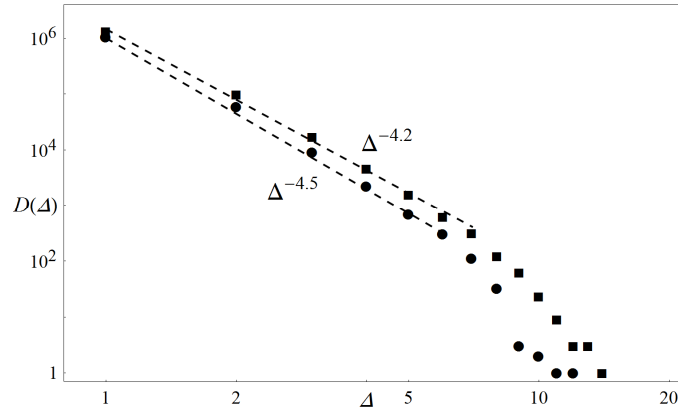
Fig. 8. Avalanche size distributions in 1D system for LLS variants: load transfer
to two nearest neighbours (squares), load transfer to one nearest neighbour (circles).
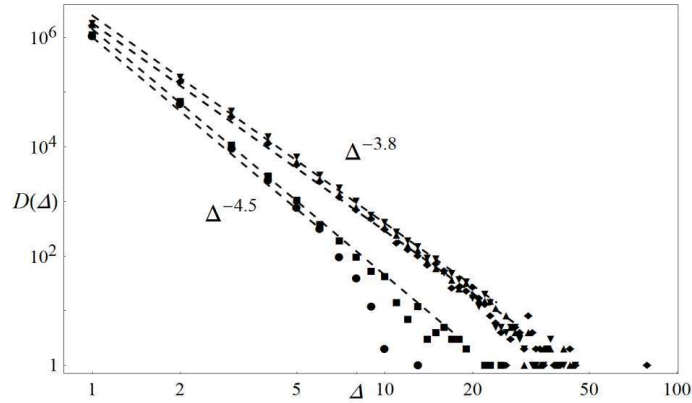Simulation results are based on 1000 samples, each containing $N = 10^4$ pillars

Fig. 9. Avalanche size distributions in 2D system for LLS variants - load transfer to:
one nearest neighbour (circles), two nearest neighbours (squares), three nearest
neighbours (diamonds), four nearest neighbours (up triangle), five nearest neighbours
(down triangle). Simulation results are based on 1000 samples, each containing
$N = 10^4$ pillars

In order to get a closer look at the distribution of avalanches for the LLS rule, we have performed 200 000 simulations for a one-dimensional system of size $N = 10^4$. It appears that the resulting avalanche distribution is in fact exponential, see Figure 10, and this is in accordance with the work by Kloster *et al.* (1997) [5, 6].

In the following we analyze the correlation between the size of the catastrophic avalanche Δ_{fa} and the total critical load F_c. As a measure of this correlation, we use Pearson's coefficient defined as

$$\rho_{\Delta_{fa},F_c} = \frac{\text{cov}(\Delta_{fa}, F_c)}{\sigma_{\Delta_{fa}}\sigma_{F_c}} \tag{2}$$

Here, $\sigma_{\Delta_{fa}}, \sigma_{F_c}$ are the corresponding standard deviations. We get the following values $\rho^{LLS} = -0.943$ and $\rho^{GLS} = 0.165$, in the LLS and the GLS models, respectively. For GLS, we can say that the correlation is negligible or does not exist. It is in contrast to the LLS rule for which there is a strong negative correlation. Graphically it has been shown in Figures 11 and 12.
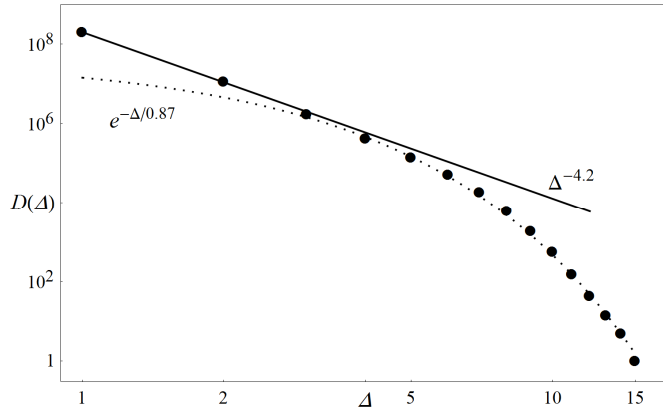

Fig. 10. Avalanche size distribution in 1D system for LLS with load transfer to one right neighbour. Figure is based on 200 000 samples, each containing $N = 10^4$ pillars
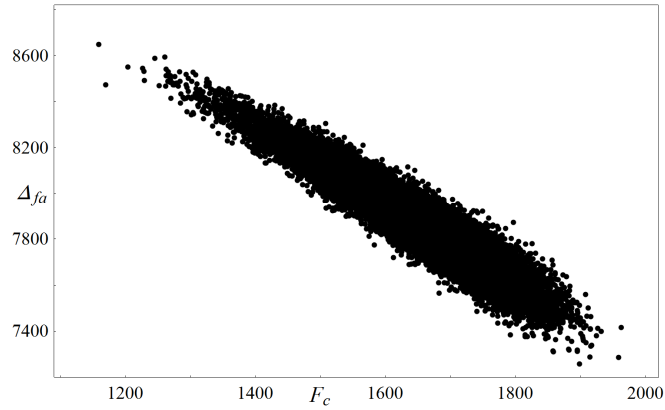

Fig. 11. Size of final catastrophic avalanche Δ_{fa} vs. total critical force F_c in 2D system for LLS rule. Figure is based on 30 000 samples, each containing $N = 10^4$ pillars
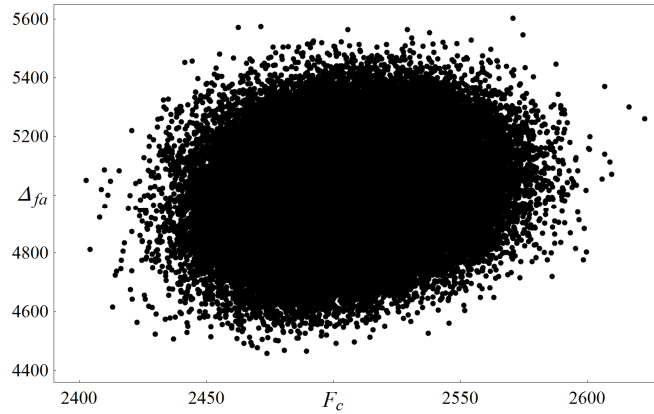
Fig. 12. Size of final catastrophic avalanche Δ_{fa} vs. total critical force F_c for GLS.

Figure is based on 100 000 samples, each containing $N = 10^4$ pillars

Discussion

We have studied the avalanche size distribution for quasi-statically loaded sets of pillars. Three different load transfer rules have been considered. For both the GLS and VLS models the avalanche distribution follows a power law, by contrast for the LLS model, the avalanche distribution is exponential.

In the present work, the values of critical stresses and sizes of catastrophic avalanches have been analysed. These results are presented for one size of the system. Work concerning the dependence of critical stress values and catastrophic avalanche sizes in relation to different system sizes for the LLS model is in preparation.

Finally we have noticed a strong negative correlation between the size of the final avalanche and the critical load in the LLS model, whereas for the GLS model there is rather no correlation between these two quantities.

References

[1]   Herrmann H.J., Roux S. (eds.), Statistical Models for the Fracture of Disordered Media, North Holland, Amsterdam 1990 and references therein.

[2]   Alava M.J., Nukala P. K.V.V., Zapperi S., Statistical models of fracture, Advances in Physics 2006, 55, 349-476.

[3]   Hemmer P.C., Hansen A., The distribution of simultaneous fiber failures in fiber bundles, ASME J. Appl. Mech. 1992, 59, 909-914.

[4]   Hansen A., Hemmer P.C., Burst avalanches in bundles of fibers: Local versus global load-sharing, Physics Letters A 1994, 184(6), 394-396.

[5]   Kloster M., Hansen A., Hemmer P.C., Burst avalanches in solvable models of fibrous materials, Phys. Rev. E 1997, 56, 2615-2625.

[6]   Pradhan S., Hansen A., Chakrabarti B.K., Failure processes in elastic fiber bundles, Rev. Mod. Phys. 2010, 82, 499-555.

[7]   Moreno Y., Gomez J.B., Pacheco A.F., Fracture and second-order phase transitions, Phys. Rev. Letters 2000, 85, 2865-2868.

[8]   Gomez J.B., Moreno Y., Pacheco A.F., Probabilistic approach to time-dependent load-transfer models of fracture, Phys. Rev. E 1998, 58, 1528-1532.

[9]   Moreno Y., Gomez J.B., Pacheco A.F., Phase transitions in load transfer models of fracture, Physica A 2001, 296, 9-23.

[10]   Raischel F., Fibre Models for Shear Failure and Plasticity, PhD thesis, University of Stuttgart 2007.

[11]   Raischel F., Kun F., Herrmann H.J., Fiber bundle models for composite materials, Conference on Damage in Composite Materials 2006, Stuttgart 2006.

[12]   Kun F., Raischel F., Hidalgo R.C., Herrmann H.J, Extensions of Fibre Bundle Models, Lecture Notes in Physics 2006, 705/2006, 57-92.

[13]   Pradhan S., Hemmer P.C., Breaking rate minimum predicts the collapse point of over-loaded materials, Phys. Rev. E 2009, 79, 41148-41152.

[14]   Pradhan S., Can we predict the failure point of a loaded composite material? Computer Physics Communications 2011, 182(9), 1984-1988.

[15]   Pradhan S., Hansen A., Hemmer P.C., Crossover behavior in burst avalanches of fiber bundles: Signature of imminent failure, Phys. Rev. Lett. 2005, 95, 125501-125504.

[16]   Pradhan S., Chakrabarti B.K., Precursors and prediction of catastrophic avalanches, Modelling Critical and Catastrophic Phenomena in Geoscience: A Statistical Physics Approach, Springer, Berlin 2006.

[17]   Hope S.M., Hansen A., Burst distribution in noisy fiber bundles and fuse models, Physica A 2009, 388, 4593-4599.

[18]   Pradhan S., Hansen A., Hemmer P.C., Burst statistics as a criterion for imminent failure, IUTAM Bookseries 2009, 10, 165-175.

[19]   Kun F., Zapperi S., Herrmann H.J., Damage in fiber bundle models, Eur. Phys. J. B 2000, 17, 269-279.

[20]   Hemmer P.C., Hansen A., Pradhan S., Rupture processes in fiber bundle models, Lecture Notes in Physics 2006, 705, 27-55.

[21]   Derda T., Domański Z., Damage evolution on two-dimensional grids - comparison of load transfer rules, Scientific Research of the Institute of Mathematics and Computer Science 2010, 1(9), 5-15.

[22]   Okabe A., Boots B., Sugihara K., Spatial Tessellations: Concepts and Applications of Voronoi Diagrams, John Wiley & Sons, England 1992.